Hindawi
Advances in Materials Science and Engineering
Volume 2021, Article ID 4625972, 11 pages
https://doi.org/10.1155/2021/4625972

Research Article

Performance of Cracked Ultra-High-Performance Fiber-Reinforced Concrete Exposed to Dry-Wet Cycles of Chlorides

Longlong Niu and Shiping Zhang

Department of Architecture Civil Engineering, Nanjing Institute of Technology, Nanjing, China

Correspondence should be addressed to Shiping Zhang; zhangshiping1982@hotmail.com

Received 11 July 2021; Revised 22 October 2021; Accepted 28 October 2021; Published 30 November 2021

Academic Editor: Luís Evangelista

This paper presents an experimental study on the performance of cracked ultra-high-performance fiber-reinforced concrete (UHPC) exposed to dry-wet cycles of 3.5% NaCl solution under the temperature of 60°C. The results show that the wider the crack, the higher the corrosion degree of steel fibers embedded in UHPC, and the deeper the chloride ion diffusion on both sides of the crack. With the increase of dry-wet cycles, the flexural strength of precracked UHPC first decreases and then increases, and the lowest flexural strength was observed in 60 dry-wet cycles. Although self-healing is hard to cease the corrosion of steel fibers, it can relieve the corrosion of steel fibers and improve the flexural strength exposed to 100 dry-wet cycles.

1. Introduction

The ultra-high-performance fiber-reinforced concrete (UHPC) has received considerable attention from researchers as a construction material owing to its excellent mechanical strength, durability, fatigue resistance, and toughness [1–5]. However, under the effect of various environmental factors, such as temperature, humidity, and external load, UHPC structure used in engineering has a possibility of generating cracks. Therefore, numerous studies have been conducted to evaluate the performance of cracked UHPC.

Beglarigale and Yazici [6] found that when the steel fibers embedded in UHPC were sufficiently covered by concrete and subjected to 1200 dry-wet cycles in artificial seawater, there was no corrosion. Shaheen and Shrive [7] believed that the corrosion of steel fibers in the UHPC matrix proceeded very slowly, only resulting in corrosion of the exposed steel fibers. Abbas et al. [8] reported that the corrosion of steel fibers in UHPC was only limited to the surface, and there was no degradation of mechanical properties after being exposed to chloride ion solutions for 6 months.

Some research [9, 10] pointed out that corrosion of steel fibers whose diameter is smaller than 0.15–0.20 mm was limited, and reductions of the residual-tensile strength could be neglected. Yoo et al. [11] thought that the steel fibers embedded in the cracked UHPC were severely corroded after being immersed in the NaCl solution. The longer the immersion duration, the higher the corrosion degree. The steel fibers corroded cracks have a significant impact on the tensile properties and durability of UHPC. Although cracks will reduce the performance of concrete, such as strength loss and steel fiber corrosion, some scholars have found that the cracked concrete has a certain degree of healing phenomenon. Yoo et al. [12] found that the steel fibers incorporated in the cracked UHPC matrix could be corroded, increasing their tensile performance due to increased surface roughness. Similarly, Mohammad et al. [13] observed the phenomenon of improvement of flexural strength of concrete by self-healing and steel fibers corrosion. Granger et al. [14] found that while using the method of water curing, the higher flexural strength of precracked UHPC could be achieved than that of air curing due to a large quantity of unhydrated cement.

Table 1: Chemical composition of Material.

Material	Chemical composition (wt%)									
	SiO_2	CaO	Fe_2O3	Al_2O3	MgO	K_2O	Na_2O	SO3	Loss	Total
Cement	20.16	63.26	3.38	4.65	0.92	0.54	0.18	1.09	3.11	97.29
Fly ash	55.54	3.64	5.09	29.41	0.82	1.04	0.63	0.48	2.99	99.64
Silica fume	92.13	0.73	0.21	0.57	0.64	0.85	0.64	0.46	3.25	99.48

Kim et al. [15] reported that the 3-day air curing was enough to recover the flexural strength of UHPC, and $CaCO_3$ was confirmed to be a kind of effective crack filling material. Granger et al. [14] investigated the effects of the recuring regime on self-healing and found that the initial stiffness of the precracked beams was recovered, and newly formed crystals developed only after recuring in water. Kwon et al. investigated the effect of self-healing on the air permeability of precracked UHPC and found that air permeability was recovered due to the precipitation of calcium carbonate inside cracks and water recuring.

The self-healing and steel fiber corrosion of UHPC has been studied separately thus far. In papers, although the effect of steel fibers corrosion on the mechanical property of UHPC was evaluated, the self-healing phenomenon was not considered. Some researchers pay attention to the effect of self-healing on the mechanical properties or durability of UHPC without considering the corrosion of steel fiber. However, cracks in UHPC could be self-healed with the moisture and carbon dioxide (CO_2) in the atmosphere. The effect of self-healing of UHPC on corrosion of steel fiber and mass transport needs to be investigated and analyzed, especially for partial self-healing. This research focused on the corrosion of steel fiber, mechanical strength, and self-healing of precracked UHPC with the crack width of 0.15 mm, 0.3 mm, and 0.5 mm exposed to dry-wet cycles of 3.5% NaCl solution for 0, 15, 30, 60, and 100 dry-wet cycles. The effect of self-healing UHPC on corrosion of steel fiber and mechanical strength was discussed from mass transport.

2. Experimental Program

2.1. Material Characterization. In this research, P·II 52.5 Portland cement produced by Jiangnan-Onoda Cement Co., Ltd., was used. The chemical composition of Portland cement, Fly ash, and Silica fume are shown in Table 1. Besides, natural siliceous sand with particles sizes of 0.08–4.75 mm and a fineness modulus of 2.6 was used as the aggregate. The adopted water-reducing admixture is a kind of powdered polycarboxylate superplasticizer, and the water is ordinary tap water. In this research, straight steel fibers coated by brass were used, and their geometrical and physical properties are shown in Table 2.

2.2. Testing Program

2.2.1. The Preparation of UHPC Specimen. A high-speed mixer was used to make UHPC. Firstly, all the dry ingredients and superplasticizer were premixed for 5 min to disperse them sufficiently. Then, the water was added and mixed for another 10 min. Finally, steel fibers were carefully added to be stirred for 5 min to make it disperse in the matrix effectively. Table 3 shows the details of the proportion of the UHPC specimens.

As shown in Figure 1, the slump flow and slump flow losses of fresh UHPC mixture were measured to be approximately 770 mm and 50 mm, which is an acceptable range of self-compactness according to the Standard GB/T50080-2016. Sump flow losses were calculated according to the difference between the initial sump flow value and 60 min sump flow value. In this study, all UHPC specimens were made in the size of 40 mm × 40 mm × 160 mm. The fresh UHPC mixture was transferred into the molds without vibration; then they were covered by wet plastic after casting 20 ± 3°C and demolded after 24 h. Finally, they were cured at the temperature of 60 ± 2°C for 3 d.

2.2.2. Preparation of Precracked UHPC Specimen. To evaluate the performance of cracked UHPC exposed to dry-wet cycles of chlorides, the specimens were preloaded to generate cracks through the side three-point bending. According to the monitorization using the crack width measuring instrument, the three-point bending loading was applied at a rate of 0.1 KN/s until the crack widths reached 0.15 mm, 0.3 mm, and 0.5 mm, i.e., ranging from 0.14 to 0.16 mm, 0.26 to 0.34 mm, and 0.46 to 0.54 mm. The specimen with crack width of 0.15 mm, 0.3 mm, and 0.5 mm marked W15, W30, and W50, respectively. It needs to be noted that, even for the same precracked specimens, the width of the cracks varied with the location. During the test, the casting face of UHPC shall be placed forward and the location of the applied load was marked on the loaded face. The preloaded test setup is shown in Figure 2. The span of pin support in the loading test setting is 100 mm.

2.2.3. Exposure Setup. In order to reduce the effect of other faces on the precrack face, the other surfaces were coated with epoxy resin except for the precrack face exposed, as shown in Figure 3. To evaluate the performance of cracked UHPC after exposing to dry-wet cycles of chlorides, the specimens were exposed to the dry-wet cycles of 3.5% NaCl solutions for 16 h and air 8 h, respectively, and the temperature was 60°C.

The dry-wet cycle test was performed in plastic containers with a volume of 60 L, of which the solid-liquid ratio is 1 : 2. The sodium chloride solution was refreshed every 15 dry-wet cycles in the first testing month and then refreshed per month until specimens were exposed to 100 dry-wet cycles. The dry-wet cycle test in the air was performed in the laboratory with a tank with 60°C and 8 h ventilation system.

Table 2: Geometrical and physical properties of steel fibers.

Diameter d_f/mm	Length l_f(mm)	Aspect ratio $[l_f/d_f]$	Tensile strength (MPa)
0.21	13	62	2869

Table 3: Mix proportion of UHPC specimens.

Cement kg/m^3	Fly ash kg/m^3	Silica fume kg/m^3	Water kg/m^3	Sand kg/m^3	Steel fiber kg/m^3	Superplastic kg/m^3
700	200	100	185	1000	140	11

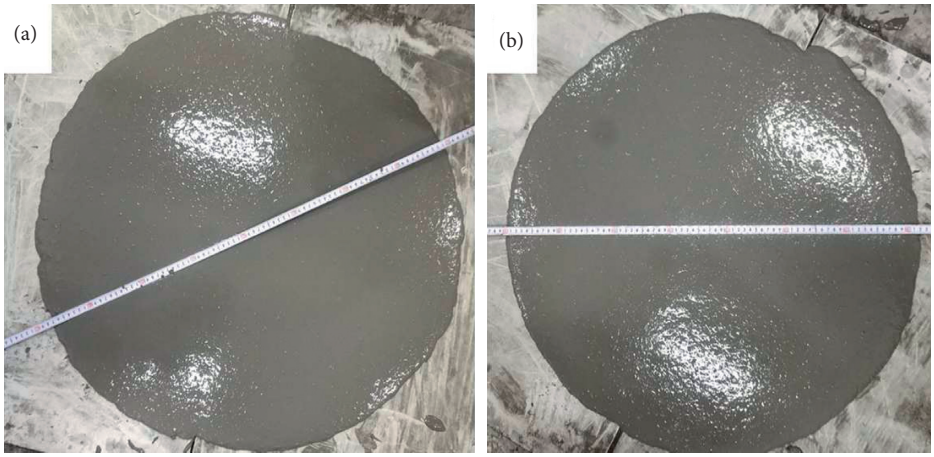

Figure 1: Slump flow. (a) Slump flow; (b) slump flow through 60 min.

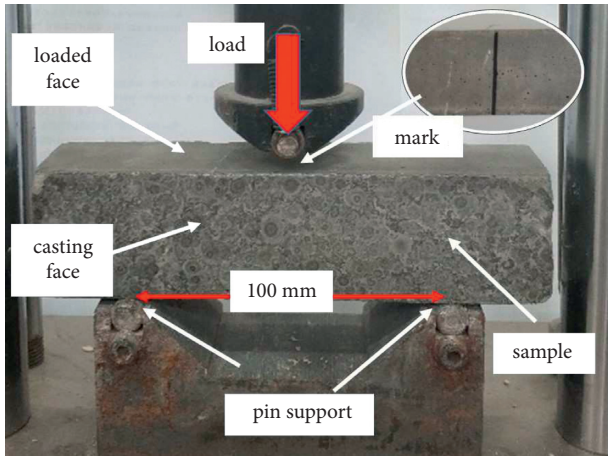

Figure 2: Preloaded test setup.

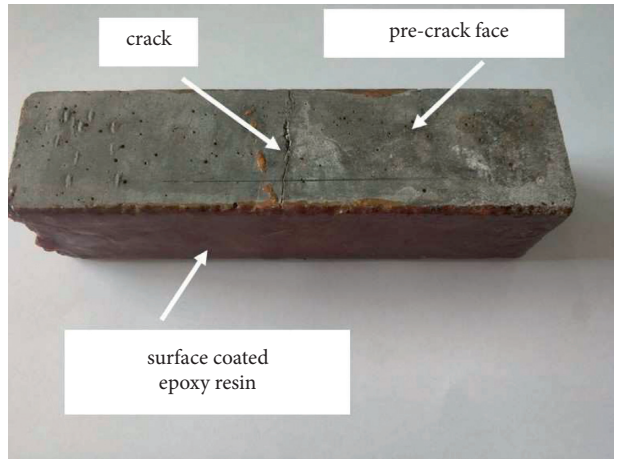

Figure 3: Surface treatment: except for the precrack face exposed, the other surfaces were coated with epoxy resin.

2.2.4. Test Procedure. In the test for compressive strength and flexural strength, the specimens were made in the size of 40 mm × 40 mm × 160 mm, and scraped surface coated epoxy resin. The compressive strength and flexural strengths of specimens were tested according to Standard GB/T17671—1999, and the flexural test for strengths loaded on the face marked (Figure 2). Water absorption testing for hardened concrete was used to evaluate the water permeability, in which specimens with the size of 40 mm × 40 mm × 160 mm were made and coated by epoxy resin according to ASTM C642. To guarantee the accuracy of the result, every test was performed on three specimens, and the mean value was adopted. To evaluate the internal structure of the UHPC specimen, an ultrasonic inspection was performed. The position of the detectors was at both ends of the prism specimen.

3. Results and Discussion

3.1. The Corrosion of Steel Fiber. Figure 4 shows the surface topography of the UHPC specimens exposed to 15, 30, 60, and 100 dry-wet cycles of chlorides. The rust spots appeared at the surface of UHPC specimens after 15 dry-wet cycles, which seems to imply that steel fibers are easy to rust when

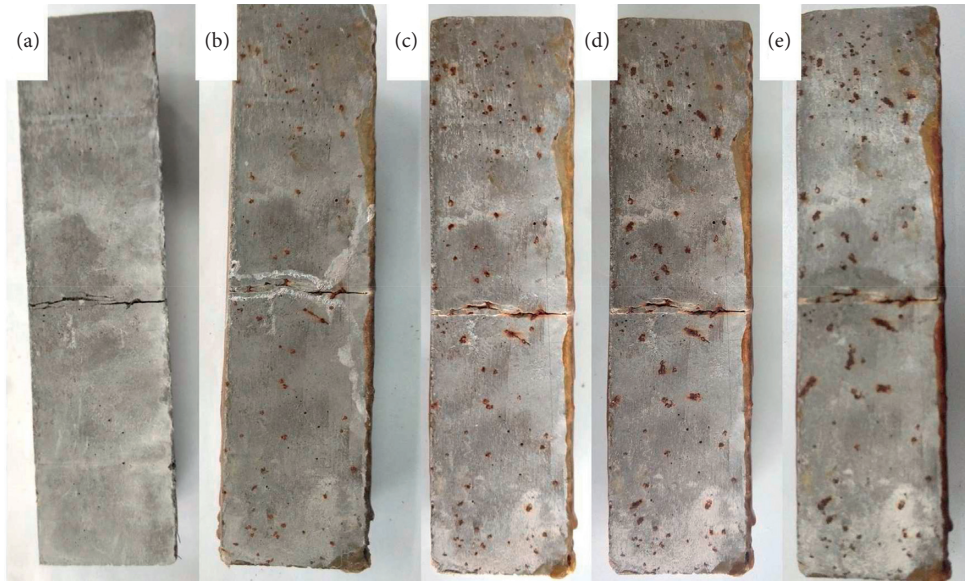

Figure 4: Surface topography of UHPC specimens: (a) the UHPC specimens unexposed to chlorides; (b–e) the UHPC specimens exposed to 15, 30, 60, and 100 dry-wet cycles of chlorides, respectively.

exposed to chloride environment. As shown in Figure 4, the UHPC specimens presented larger rust spots at the surface with the number of dry-wet cycles. It should be noted that no new rust spots appeared at the surface of the UHPC specimens after 15 dry-wet cycles, only resulting in further severe corrosion of corroded steel fibers. Although the fibers presented severe corrosion after 100 dry-wet cycles, the damage was not extended and lead to cracking or spalling of the adjacent matrix caused by fiber corrosion. This may be because of the weak expansion stress caused by the small fiber diameter and the strength matrix [16].

In order to evaluate the corrosion of steel fiber, the specimens were broken along the precrack (middle position), and then the specimen of the fracture face was observed. Figure 5 shows the corrosion of steel fibers of UHPC specimens after 100 cycles of drying and wetting. It was observed that the fibers interior, the uncracked section of UHPC, did not present any signs of corrosion after 100 dry-wet cycles. As shown in Figure 5, with the increase of crack width, the corrosion of steel fibers became more serious. For the UHPC specimens with the crack width of 0.15 mm, the fibers within 10 mm close to the surface presented rust spots at the surface and did not rupture while pulling out. There were rust spots of the fibers in the whole fracture face of the precracked specimen with the crack width of 0.3 mm and 0.5 mm. Besides, the closer to the surface, the more serious the corrosion. For the UHPC specimens with the crack width of 0.3 mm and 0.5 mm, the fibers in fracture face presented large pits and rupture while pulling out (Figures 5: marked with a white circle).

In order to evaluate the chloride diffusion along the crack of precracked UHPC, 0.1 mol/l $AgNO_3$ solution was sprayed on the fracture face. Figure 6 shows the distribution of chloride on the fracture face after 100 dry-wet cycles. When $AgNO_3$ solution was sprayed on the fracture face, there was no white precipitate on the uncracked UHPC section. This phenomenon indicates that there is almost no penetration of chloride solution. By contrast, the white precipitate appeared near the exposed area of UHPC specimens with the crack width of 0.15 mm, indicating the permeation of chloride solution. A large amount of white precipitate appeared on the UHPC specimens with width of the 0.3 mm–0.5 mm, which indicates that chloride ions entered into the specimens through cracks and led to steel fibers corrosion, and with the increase of crack width, the more the steel fibers were exposed to the corrosive solution, and the corrosion degree was also increased.

The specimens were cut with a cutting machine, then sprayed with 0.1 mol/l $AgNO_3$ solution to evaluate the depth of chloride diffusion. Figure 7 shows the depth of chloride diffusion after 100 dry-wet cycles. The uncracked and precracked UHPC specimens showed about 1 mm width of white precipitates area at the bottom, but there was no obvious white precipitate in the fracture face of the uncracked and precracked specimen with the crack width of 0.15 mm exposed to100 dry-wet cycles of corrosive solution. For the precracked specimen with the crack width of 0.3 mm and 0.5 mm, the white precipitate area with the width of 1.5 mm and 8 mm, respectively, appeared on the cut face, as shown in Figure 7. This indicated that chloride ion was difficult to enter the uncracked specimens, but the pulling out of fiber would lead to fiber-matrix interface damage; i.e., larger crack widths induce larger damage at the fiber-matrix interface and a greater exposed area of the steel fiber [17], accelerating chloride ion into the concrete. Some researchers [10, 18] observed localized corrosion damage at the hook and the intersecting part between fiber and crack.

3.2. Mechanical Performance. In this study, compressive strength tests were performed on prism uncracked specimens with the size of 40 mm × 40 mm × 160 mm. Figure 8 shows the

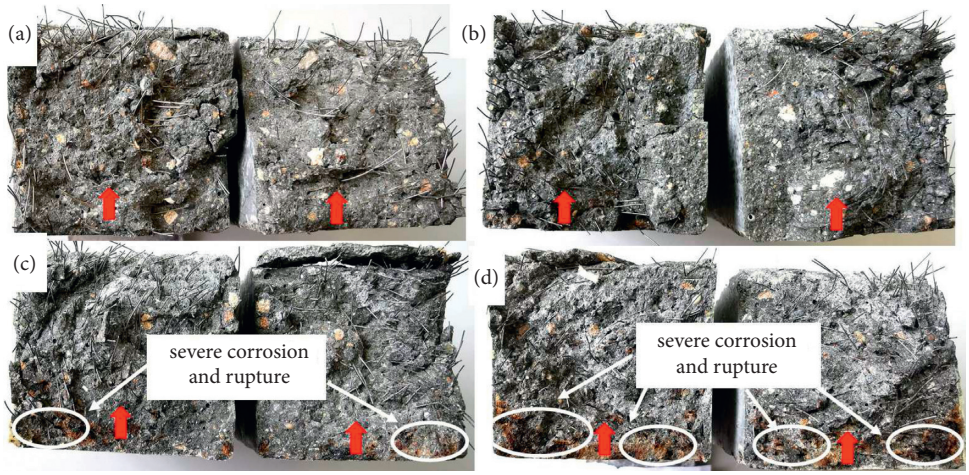

Figure 5: The corrosion of steel fibers of UHPC specimens after 100 cycles of drying and wetting: (a–d) the crack width 0, 0.15 mm, 0.3 mm, and 0.5 mm. The arrow indicates the direction of solution erosion.

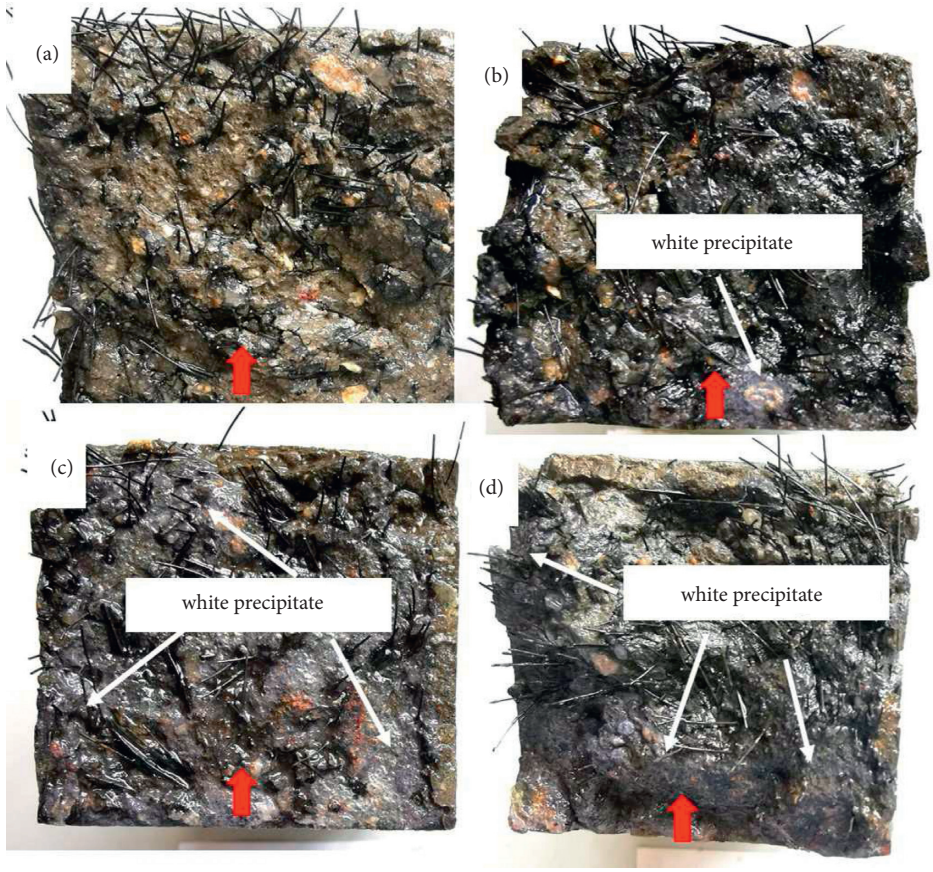

Figure 6: Distribution of chloride on the fracture face: the fracture face sprayed 0.1 mol/l $AgNO_3$ solution: (a-d) the crack width 0, 0.15 mm, 0.3 mm, and 0.5 mm. The arrow indicates the direction of solution erosion.

compression test results after 100 dry-wet cycles. It was observed that the compressive strength only slightly increased with curing time, and it was increased by 8.7%, 11.6%, and 9.6%, respectively, after 30, 60, and 100 dry-wet cycles. On the 60th dry-wet cycles, the concrete reached the highest compressive strength level, which was approximately 192 MPa, and then the compressive strength was nearly a constant.

Figure 9 shows the test results of flexural strength after 100 dry-wet cycles, and it can be seen that as the crack width increased, the flexural strength gradually decreased, and the flexural strength was decreased by 5.0%, 11.3%, and 16.4% for the crack width of 0.15 mm, 0.3 mm, and 0.5 mm, respectively. It should be noted that whether the specimen is cracked or not, the flexural strength of the specimen before curing is

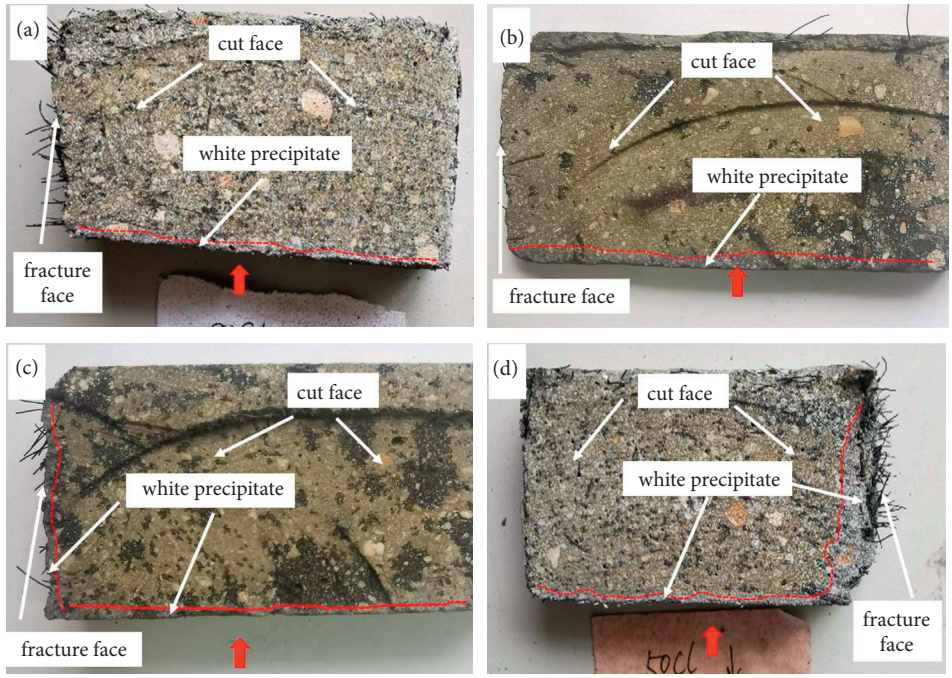

Figure 7: Depth of chloride diffusion: the cut face sprayed 0.1 mol/l $AgNO_3$ solution: (a–d) the crack width 0, 0.15 mm, 0.3 mm, and 0.5 mm. The arrow indicates the direction of solution erosion.

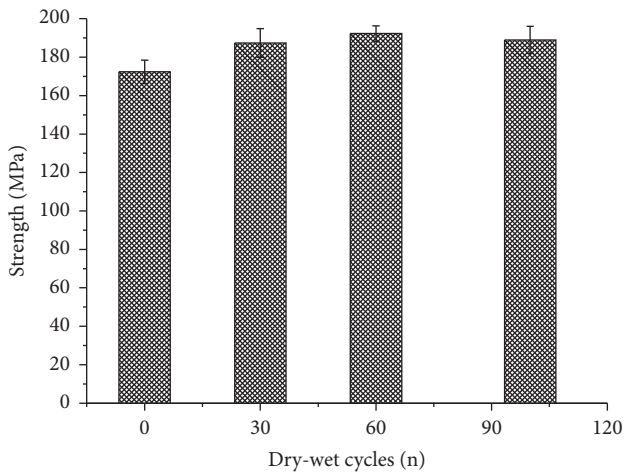

Figure 8: Change of compressive strength of specimens with dry-wet cycles.

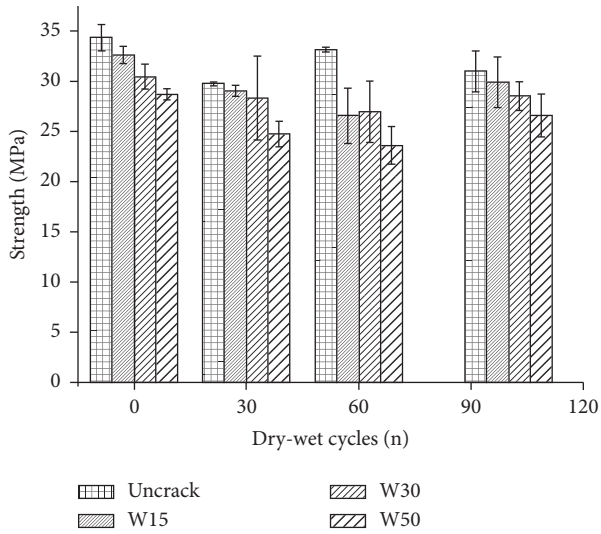

Figure 9: Change of flexural strength of specimens with dry-wet cycles.

higher. These results show that, generally, the change of flexural strength for uncracked UHPC can be ignored considering the effect of fiber dispersion. The flexural strength of precrack UHPC decreased and then increased. The lowest flexural strength was observed in 60 dry-wet cycles. Based on the literature [19], the self-healing and the increase roughness may increase the fibers-matrix frictional bond, which explain the improved residual-flexural strength.

It should be noted that although there was no significant decrease in flexural strength after 100 dry-wet cycles, once the steel fibers corrosion initiates, the corrosion is hard to be ceased, which would result in a progressive and localized reduction of the fiber cross section. Once a critical cross section is reached (i.e., the tensile capacity of the steel is lower than the fiber-matrix bond strength), the failure mode of the UHPC would change from fiber pull out to fibers yield, and the residual strength would decrease [20].

3.3. Self-Healing. The mass of water absorbed was measured at regular intervals. The average water absorption per unit area of specimen is reported in Figure 10. As illustrated in Figure 10 for concrete unexposed, the water absorption of uncracked specimens was 0.18 kg/m^2, but it was increased to 0.38 kg/m^2, 0.30 kg/m^2, to 0.32 kg/m^2 for precracked

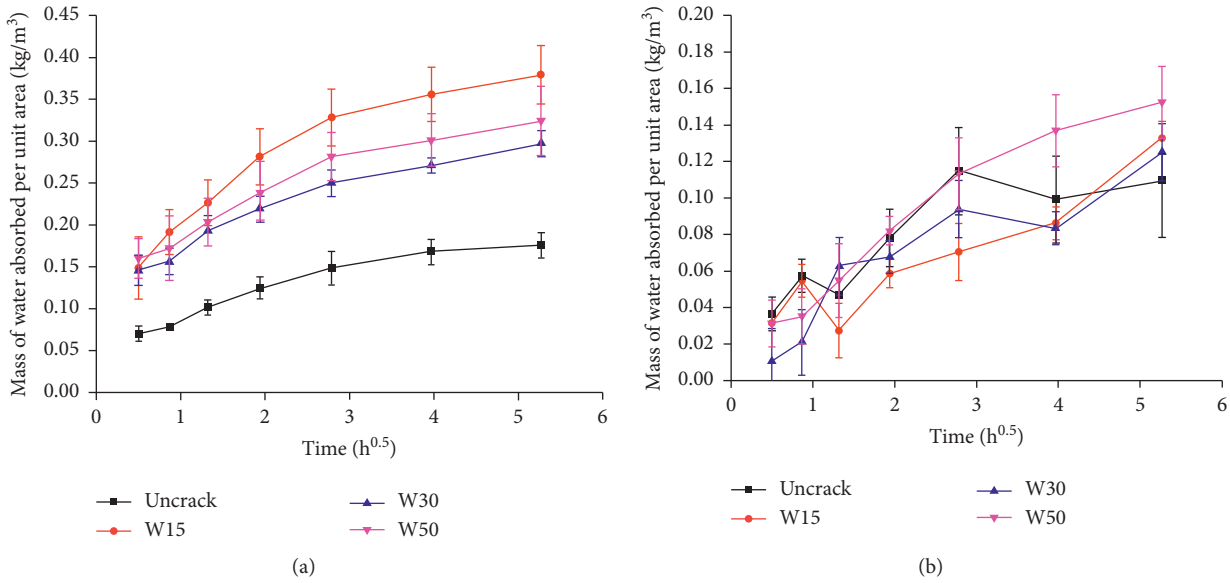

Figure 10: Water absorption of specimens. (a) 0 dry-wet cycles. (b) 100 dry-wet cycles.

specimens with the crack width of 0.15 mm, 0.3 mm, and 0.5 mm, respectively. The water absorption reached the highest for the crack width of 0.15 mm, which is approximately two times that of the uncracked specimens. These results show no significant difference for the water absorption of precracked specimens among 0.15 mm, 0.3 mm, and 0.5 mm after 100 dry-wet cycles, indicating that cracks of precracked specimens were filled. The absorption coefficient of the specimens shown in Figure 11 shows that the increase of crack width caused the increase in the water absorption coefficient, and the maximum water absorption coefficient was observed when the crack width was 0.15 mm. After 100 dry-wet cycles, the absorption coefficient of precracked specimens was kept as a constant, which is attributed to the rehydration of cement, the pozzolanic reaction of silica fume, and the formation of $CaCO_3$ [15, 20–22].

The ultrasonic velocities of the concrete specimens were measured along the longitudinal direction; all test specimens were dried at 105°C for 24 h until saturation, avoiding the dispersion of results due to the humidity variation of the specimens. Figure 12 shows the results of the ultrasonic velocity of the concrete specimens, and it can be seen that the ultrasonic velocity decreased with the crack width and increased with the number of dry-wet cycles. The results also showed that the curing of dry-wet cycles had slightly improved ultrasonic velocity. The increase of ultrasonic velocity means the decrease of porosity [23]. It was revealed that self-healing of precrack of UHPC might improve the internal compactness of concrete through rehydration of unhydrated cement, and formation of calcium carbonate, thus resulting in a high ultrasonic velocity.

Figures 13–15 show changes of crack of precrack of UHPC specimens with width 0.15 mm, 0.3 mm. and 0.5 mm, separately. According to Figures 13–15, it can be known that regardless of the crack width, all the cracks in the UHPC were fully or partially self-healed. The cracks with a width smaller than or equal to 0.08 mm were fully filled with self-healing products after 30 cycles of dry-wet. The crack width of 0.15 mm was mostly filled with the products so that almost all of the cracks seemed to be well self-healed, as shown in Figure 13. The crack with width 0.3 mm decreased by about 30% and was only partially filled with the self-healing, as shown in Figure 14. There is little change in the crack for the precrack UHPC with a crack width of 0.5 mm, as shown in Figure 15. White products of self-healing were not observed on the crack surface (Figures 14 and 15), which means that, during the self-healing process, the products may preferentially deposit inside the crack. Although Figures 14 and 15 show less change of crack of precrack of UHPC specimens with width 0.3 mm and 0.5 mm, the water absorption and ultrasonic wave showed that self-healing might occur inside the crack. This result implies the partial self-healing of precrack of UHPC specimens with width 0.3 mm and 0.5 mm. The partial self-healing can delay the corrosion progress, but it is hard to cease in a long term perspective.

3.4. The Deterioration and Recovery Mechanisms. The steel fibers are easy to rust while exposed to chloride environment, as shown in Figure 4. The transport of ions and moisture through the matrix surrounding the crack and along the fibers bridging the crack leads to corrosion of the steel fibers bridging the crack (Figure 5) and dissolution of the hardened cement paste, which would reduce the effective cross section of the fiber corroded and the fiber-matrix bond strength. Therefore, the flexural strength of the precracked UHPC decreased.

Figure 9 shows the flexural strength of the precracked UHPC decreased first and then increased after 100 dry-wet cycles, and the lowest flexural strength was observed in 60 dry-wet cycles. These observations do not fully agree with former deterioration hypotheses that associate changes in the mechanical performance primarily to fiber corrosion

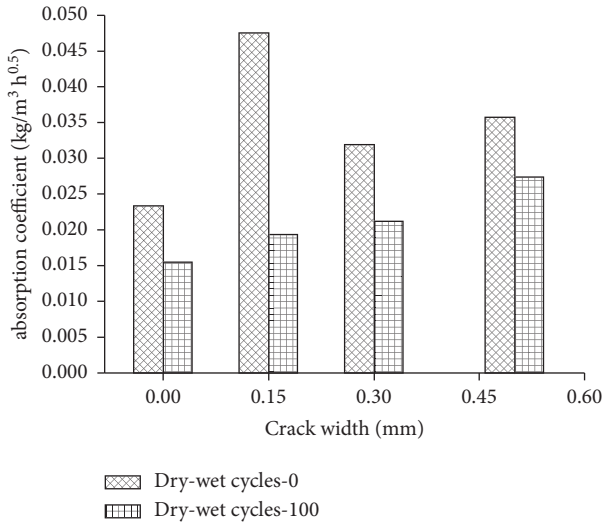

Figure 11: The absorption coefficient of specimens.

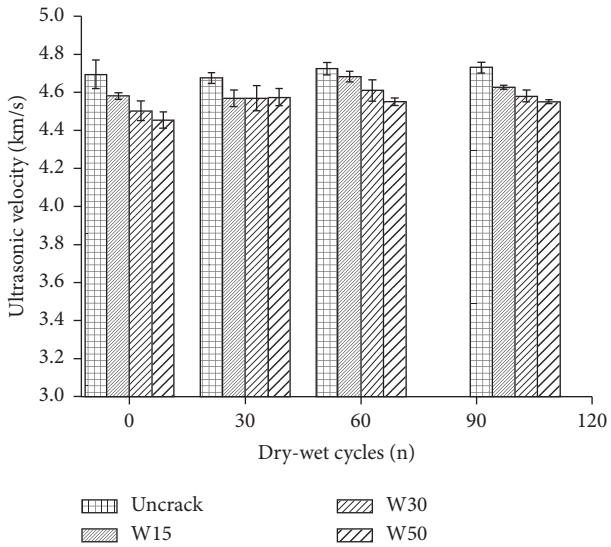

Figure 12: Results of the ultrasonic velocity of specimens.

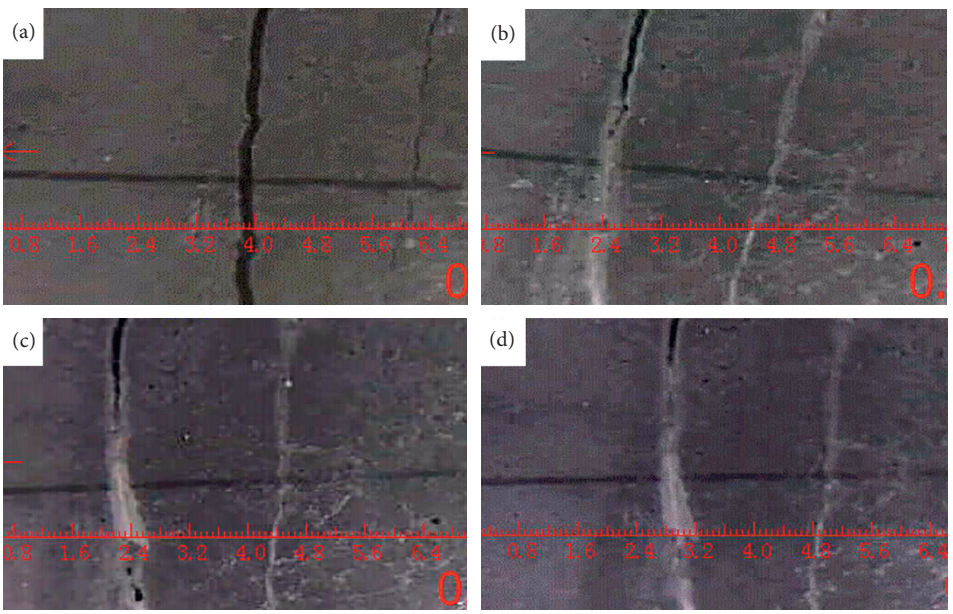

Figure 13: Change of crack of the precrack UHPC with width 0.15 mm: (a) the UHPC specimens unexposed to chlorides; (b–d) the UHPC specimens exposed to 30, 60, and 100 dry-wet cycles of chlorides, respectively.

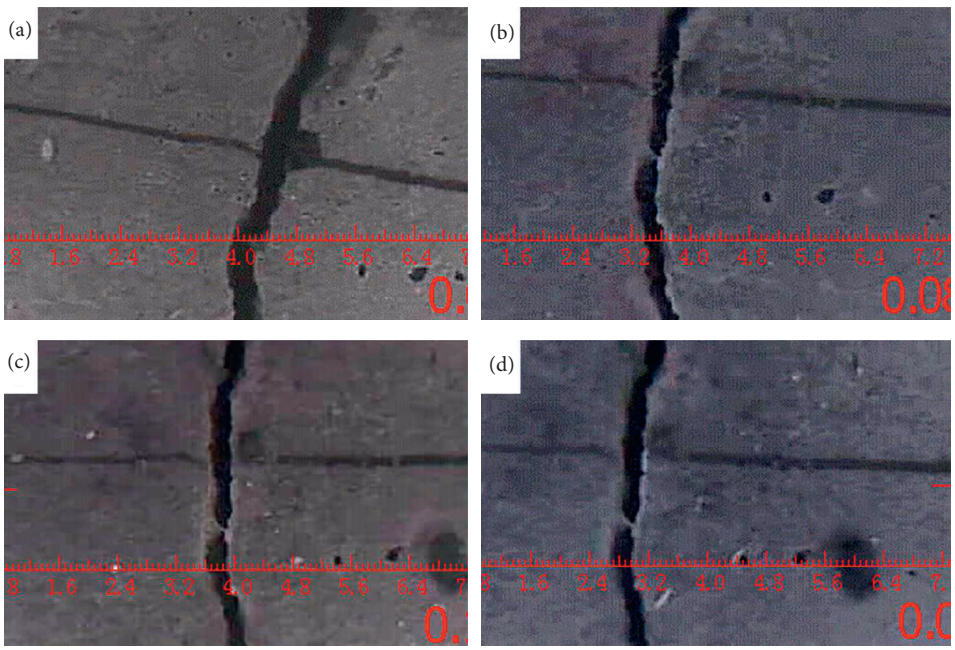

Figure 14: Change of crack of the precrack UHPC with width 0.3 mm: (a) the UHPC specimens unexposed to chlorides; (b–d) the UHPC specimens exposed to 30, 60, and 100 dry-wet cycles of chlorides, respectively.

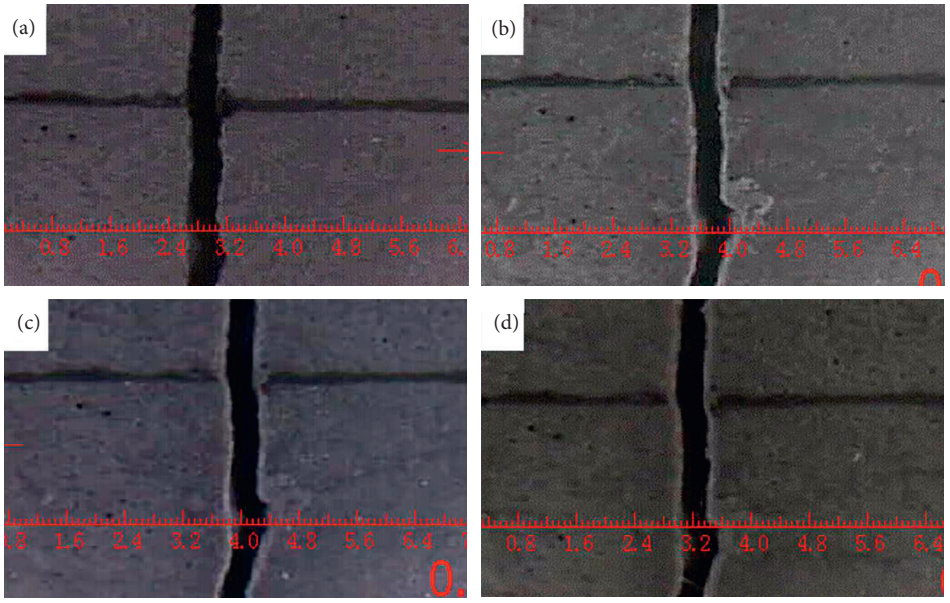

Figure 15: Change of crack of the pre-crack UHPC with width 0.5 mm: (a) the UHPC specimens unexposed to chlorides; (b–d) the UHPC specimens exposed to 30, 60, and 100 dry-wet cycles of chlorides, respectively.

[10]. Therefore, more processes that affect its performance need to consider besides fiber corrosion.

Due to rehydration and carbonation in the hardened cement paste, the cracks were filled and self-healed with time (Figure 13), therefore which reducing substantially mass transport (Figures 10–12) and then corrosion of steel fibers. Based on studies [16, 17], self-healing may be responsible for increase in the residual performance of the cracked composite, which explain the improved residual-flexural strength after 100 dry-wet cycles.

The precracked UHPC, with a width of approximately 0.3 mm or larger, presented serious corrosion after 100 dry-wet cycles (Figures 5 and 6). Once the corrosion initiates, the partial self-healing is hard to cease the corrosion progress. It can be predicted that the performance would deteriorate for partial self-healing UHPC under long-term corrosive exposures. Further research on quantifying the corrosion of the steel fibers and self-healing process inside cracks is needed to understand the long-term impact of corrosive exposures on the performance of precracked UHPC.

4. Conclusions

In this study, the performance of precracked UHPC exposed to dry-wet cycles of chlorides was analyzed. The corrosion of steel fiber, mechanical performance, and self-healing of precracked UHPC with chloride erosion were evaluated. The effect of self-healing UHPC on corrosion of steel fiber and mechanical strength was discussed from mass transport. The following conclusions can be drawn:

(1) There are the depth of chloride intrusion about 1 mm, only corrosion of steel fibers located on the exposed surface, and no substantial damage to uncracked UHPC after being immersed in the 3.5% NaCl solution for 100 dry-wet cycles.

(2) With the increase of crack width in precracked UHPC, the fiber corrosion becomes more serious, and the closer to the surface, the corrosion degree of steel fiber was higher. The fiber-matrix interface damage due to pull outing of fibers accelerate chloride ion into the concrete.

(3) The flexural strength of the precracked UHPC decreased first and then increased after 100 dry-wet cycles, and the lowest flexural strength was observed in 60 dry wet cycles. This may be due to the self-healing and the surface roughness of steel fibers from the corrosion increased.

(4) The cracks with a width of approximately 0.15 mm or smaller were completely self-healed, while the widest cracks, with a width of approximately 0.3 mm or larger, were partially healed. Self -healing can reduce chloride erosion and relieve the corrosion of steel fibers, but it was hard to cease the corrosion of steel fibers, especially partial self-healing. It can be predicted that the performance would deteriorate for partial self-healing UHPC under long-term corrosive exposures.

Data Availability

The experimental data used to support the observations of this study are included in the article.

Conflicts of Interest

The authors declare that they have no competing interests.

Acknowledgments

This work was supported by the Natural Science Foundation of China (Grant nos. 52078247 and 51678292) and Six Talent Peaks Project in Jiangsu Province (JZ-023).

References

[1] F. U. A. Shaikh, S. Luhar, H. S. Arel, and I. Luhar, "Performance evaluation of ultrahigh performance fibre reinforced concrete–a review," *Construction and Building Materials*, vol. 232, Article ID 117152, 2020.

[2] Y. Rui, P. Spiesz, and H. J. H. Brouwers, "Mix design and properties assessment of ultra-high performance fibre reinforced concrete (UHPFRC)," *Cement and Concrete Research*, vol. 56, no. 2, pp. 29–39, 2014.

[3] C. Gu, W. Sun, L. Guo et al., "Investigation of microstructural damage in ultrahigh-performance concrete under freezing-thawing action," *Advances in Materials Science and Engineering*, vol. 2018, Article ID 3701682, 9 pages, 2018.

[4] T. Wang, J. Gong, B. Chen et al., "Mechanical properties and shrinkage of ultrahigh-performance concrete containing lithium carbonate and nano-calcium carbonate," *Advances in Civil Engineering*, vol. 2021, Article ID 6646272, 15 pages, 2021.

[5] J. Wang and Q. Sun, "Experimental study on improving the compressive strength of UHPC turntable," *Advances in Civil Engineering*, vol. 2020, Article ID 3820756, 21 pages, 2020.

[6] A. Beglarigale and H. Yazıcı, "Electrochemical corrosion monitoring of steel fiber embedded in cement based composites," *Cement and Concrete Composites*, vol. 83, no. 10, pp. 427–446, 2017.

[7] E. Shaheen and N. G. Shrive, "Optimization of mechanical properties and durability of reactive powder concrete," *Aci Materials Journal*, vol. 103, no. 6, pp. 444–451, 2006.

[8] S. Abbas, A. M. Soliman, and M. L. Nehdi, "Exploring mechanical and durability properties of ultra-high performance concrete incorporating various steel fiber lengths and dosages," *Construction and Building Materials*, vol. 75, no. 1, pp. 429–441, 2015.

[9] P. S. Mangat and K. Gurusamy, "Permissible crack widths in steel fibre reinforced marine concrete," *Materials and Structures*, vol. 20, no. 5, pp. 338–347, 1987.

[10] J.-L. Granju and S. Ullah Balouch, "Corrosion of steel fibre reinforced concrete from the cracks," *Cement and Concrete Research*, vol. 35, no. 3, pp. 572–577, 2005.

[11] D.-Y. Yoo, J. Y. Gim, and B. Chun, "Effects of rust layer and corrosion degree on the pullout behavior of steel fibers from ultra-high-performance concrete," *Journal of Materials Research and Technology*, vol. 9, no. 3, pp. 3632–3648, 2020.

[12] D. Y. Yoo, W. Shin, and B. Chun, "Corrosion effect on tensile behavior of ultra-high performance concrete reinforced with straight steel fibers," *Cement and Concrete Composites*, vol. 109, no. 5, Article ID 103566, 2020.

[13] B. B. Mohammad, A. Fereydon, S. N. Hamed, and S. Hamed, "Effect of steel fiber and different environments on flexural behavior of reinforced concrete beams," *Applied Sciences*, vol. 7, no. 10, Article ID 7101011, 2020.

[14] S. Granger, A. Loukili, G. Pijaudier-Cabot, and G. Chanvillard, "Experimental characterization of the self-healing of cracks in an ultra high performance cementitious material: mechanical tests and acoustic emission analysis," *Cement and Concrete Research*, vol. 37, no. 4, pp. 519–527, 2007.

[15] S. Kim, D. Y. Yoo, M. J. Kim, and N. Banthia, "Self-healing capability of ultra-high-performance fiber-reinforced concrete after exposure to cryogenic temperature," *Cement and Concrete Composites*, vol. 104, no. 11, Article ID 103335, 2019.

[16] V. M. Mesona, M. Geikerd, G. Fischer et al., "Durability of cracked SFRC exposed to wet-dry cycles of chlorides and carbon dioxide–multiscale deterioration phenomena," *Cement and Concrete Research*, vol. 135, no. 9, pp. 106–120, 2020.

[17] V. Marcos-Meson, A. Michel, A. Solgaard, G. Fischer, C. Edvardsen, and T. L. Skovhus, "Corrosion resistance of steel fibre reinforced concrete–a literature review," *Cement and Concrete Research*, vol. 103, no. 1, pp. 1–20, 2018.

[18] V. Marcos-Meso, A. Solgaard, G. Fischer, C. Edvardsen, and A. Michel, "Pull-out behaviour of hooked-end steel fibres in cracked concrete exposed to wet-dry cycles of chlorides and carbon dioxide–mechanical performance," *Construction and Building Materials*, vol. 240, no. 4, Article ID 117764, 2020.

[19] C. Frazo, J. Barros, A. Cames, A. C. Alves, and L. Rocha, "Corrosion effects on pullout behavior of hooked steel fibers in self-compacting concrete," *Cement and Concrete Research*, vol. 79, no. 1, pp. 112–122, 2016.

[20] D. Yoo, W. Shin, B. Chun, and N. Banthia, "Assessment of steel fiber corrosion in self-healed ultra-high-performance fiber-reinforced concrete and its effect on tensile performance," *Cement and Concrete Research*, vol. 133, no. 7, Article ID 106091, 2020.

[21] C. Edvardsen, "Water permeability and autogenous healing of cracks in concrete," *Aci Materials Journal*, vol. 96, no. 4, pp. 448–454, 1996.

[22] D. Homma, H. Mihashi, and T. Nishiwaki, "Self-healing capability of fibre reinforced cementitious composites," *Journal of Advanced Concrete Technology*, vol. 7, no. 2, pp. 217–228, 2009.

[23] S. O. Naffa, M. Goueygou, B. Piwakowski, and F. Buyle-Bodin, "Detection of chemical damage in concrete using ultrasound," *Ultrasonic*, vol. 40, no. 5, pp. 247–251, 2002.